THE JOURNAL OF BIOLOGICAL CHEMISTRY VOL. 286, NO. 23, pp. 20861–20869, June 10, 2011
© 2011 by The American Society for Biochemistry and Molecular Biology, Inc. Printed in the U.S.A.

Novel Nucleolar Pathway Connecting Intracellular Energy Status with p53 Activation*[S]

Received for publication, December 10, 2010, and in revised form, March 14, 2011 Published, JBC Papers in Press, April 6, 2011, DOI 10.1074/jbc.M110.209916

Takuya Kumazawa[‡1], Kazuho Nishimura[‡1], Takao Kuroda[§], Wakana Ono[‡], Chie Yamaguchi[‡], Naohiro Katagiri[‡], Mai Tsuchiya[‡], Hiroshi Masumoto[‡], Yuka Nakajima[‡§], Akiko Murayama[‡§¶], Keiji Kimura[‡], and Junn Yanagisawa[‡§2]

From the [‡]Graduate School of Life and Environmental Sciences and the [§]Center of Tsukuba Advanced Research Alliance, University of Tsukuba, 1-1-1 Tennoudai, Tsukuba 305-8577 and [¶]PREST, JST, Saitama, Japan

In response to a shortage of intracellular energy, mammalian cells reduce energy consumption and induce cell cycle arrest, both of which contribute to cell survival. Here we report that a novel nucleolar pathway involving the energy-dependent nucleolar silencing complex (eNoSC) and Myb-binding protein 1a (MYBBP1A) is implicated in these processes. Namely, in response to glucose starvation, eNoSC suppresses rRNA transcription, which results in a reduction in nucleolar RNA content. As a consequence, MYBBP1A, which is anchored to the nucleolus via RNA, translocates from the nucleolus to the nucleoplasm. The translocated MYBBP1A induces acetylation and accumulation of p53 by enhancing the interaction between p300 and p53, which eventually leads to the cell cycle arrest (or apoptosis). Taken together, our results indicate that the nucleolus works as a sensor that transduces the intracellular energy status into the cell cycle machinery.

Intracellular energy balance is important for cell survival. In response to nutrient or environmental stresses that cause reduction in the intracellular energy level, mammalian cells sense the intrinsic energy status and attempt to restore bioenergetic homeostasis through compensatory changes in the regulation of intermediate metabolic processes. One such mechanism is the reduction of ribosome biosynthesis, a major biosynthetic and energy-consuming process in mammalian cells, whereas the other mechanism is the arrest of cell proliferation. The LKB1-AMP-activated protein kinase (AMPK)[3] pathway is reportedly involved in both regulatory processes (1–5). During energy starvation or glucose deprivation, when the cellular AMP/ATP ratio is increased, the LKB1-AMPK pathway is activated. This signaling in turn inhibits the mammalian target of rapamycin (mTOR)/p70 S6 kinase activity that is required for rapid and sustained serum-induced ribosomal biosynthesis (2). In addition to this regulation, AMPK, which is reportedly activated in response to reduced energy level, phosphorylates and activates p53, which leads to G_1 cell cycle arrest (6). Inhibition of mTOR by AMPK and G_1 cell cycle arrest by AMPK via p53 activation suppresses energy expenditure and protects cells from energy deprivation-induced apoptosis (4, 5).

On the other hand, a recent study in our laboratory revealed that glucose deprivation also reduces rRNA synthesis, which leads to down-regulation of ribosome biosynthesis in HeLa cells lacking the LKB1-AMPK pathway (7). We found that a novel nucleolar protein, nucleomethylin (NML), forms an energy-dependent nucleolar silencing complex (eNoSC) with SIRT1 and SUV39H1 and functions in this process. Our results suggest that an energy-dependent change in the NAD^+/NADH ratio regulates eNoSC, allowing the complex to couple the changing energy status with the level of rRNA transcription by regulating the epigenetic status of rRNA clusters. eNoSC promotes the restoration of energy balance and protects cells from energy deprivation-induced apoptosis (7).

With regard to p53 activation, several lines of evidence show that apart from ribosomal biogenesis, the nucleolus has additional functions, including regulation of mitosis, cell cycle progression, and proliferation (8), and many forms of stress response such as p53 activation (9–11). Among them, several studies have shed light on the relationship between ribosomal biogenesis and p53 activation in response to nucleolar stress; p53 is reportedly activated by the reduction in ribosomal biogenesis through inhibition of rRNA transcription and processing (12–15). Inhibition of rRNA transcription by actinomycin D or TIF-IA siRNA treatment, which suppresses ribosomal biogenesis, causes disturbance of the nucleolus (9, 15–17). The ribosome-induced nucleolar disturbance is thought to activate p53 by blocking proteasomal degradation via MDM2. This can be achieved by negative regulation of MDM2 by the tumor suppressor protein p19ARF or ribosomal proteins, both of which sequester MDM2, resulting in stabilization of p53 (18–20).

Very recently, we found that a nucleolar protein, Myb-binding protein 1a (MYBBP1A), is involved in p53 activation when ribosomal biogenesis is suppressed. MYBBP1A, which is anchored to the nucleolus through RNA, translocates from the nucleolus to the nucleoplasm when nucleolar RNA content is reduced by inhibition of rRNA transcription. The translocated MYBBP1A acetylates and accumulates p53 by facilitating the interaction between p53 and histone acetyltransferase p300 (27). Given that nutrient shortage can reduce nucleolar RNA

* This work was supported by a nuclear system to decipher operation code (DECODE) from the Ministry of Education, Culture, Sports, Science, and Technology (MEXT), Japan.

[S] The on-line version of this article (available at http://www.jbc.org) contains supplemental Fig. 1.

[1] Both authors were equal contributors.

[2] To whom correspondence should be addressed: Graduate School of Life and Environmental Sciences, University of Tsukuba, Tsukuba Science City, Ibaraki 305-8577, Japan. Tel.: 81-29-853-7320; Fax: 81-29-853-7322; E-mail: junny@agbi.tsukuba.ac.jp.

[3] The abbreviations used are: AMPK, AMP-activated protein kinase; eNOSc, energy-dependent nucleolar silencing complex; MYBBP1A, Myb-binding protein 1a; NML, nucleomethylin; mTOR, mammalian target of rapamycin; pre-rRNA, precursor rRNA; UBF, upstream binding factor.

content by suppressing rRNA transcription, MYBBP1A may cause activation of p53 that is induced by glucose deprivation.

Here we report that NML senses the energy status and reduces nucleolar RNA content by suppressing rRNA transcription in response to glucose starvation and that this leads to the translocation of MYBBP1A from the nucleolus to the nucleoplasm. Then, MYBBP1A activates p53 by enhancing its acetylation, which is a novel pathway different from the already known LKB1-AMPK pathway. These findings indicate that NML and MYBBP1A may be the sensors in the nucleolus that connect intracellular energy status with the cell cycle machinery.

EXPERIMENTAL PROCEDURES

Cell Culture and Expression Vector—MCF-7 human breast cancer cells were maintained in Dulbecco's modified Eagle's medium containing 1000 mg/liter glucose supplemented with 10% fetal bovine serum, 100 units/ml penicillin, and 100 μg/ml streptomycin. WI-38 human normal fibroblast cells were cultured in Dulbecco's modified Eagle's medium containing 4500 mg/liter glucose with 10% fetal bovine serum, 100 units/ml penicillin, and 100 μg/ml streptomycin. MCF-7 cells were transfected with expression vectors encoding the respective proteins (pcDNA3-FLAG -mouse MYBBP1A, pcDNA3-FLAG-mouse NML).

RNA Interference—For transfection of siRNAs, cells at 30–50% confluency were transfected with 20 nM siRNA using Lipofectamine RNAi max (Invitrogen) according to the manufacturer's protocol and incubated for the indicated times. All siRNAs were purchased from Invitrogen. The sequence of siRNA duplexes is as follows: AMPKα1 #1(5′-AAGAAUGGUACUCUUUCAGGAUGGG-3′), AMPKα1#2 (5′-CACAGAAGGAUUUAAAUAUUGAGGG-3′), p53 (5′-UUCCGUCCCAGUAGAUUACCACUGG-3′), MYBBP1A#1 (5′-UUCACCAGCCGACCUGACUGAAAGA-3′), MYBBP1A#2 (GGUCCGAGAUGAAAUAUGCCCUGAA), NML#1 (5′-UAGGAAGUCCCUGAUGUUGGUUCCC-3′), NML#2 (5′-ACUGCUUGCGGCUUAAUGUAUGAGG-3′). Stealth RNAi™ Luciferase reporter control duplex was used as a negative control.

Cell Cycle Analysis—Cells were harvested by trypsinization and fixed and stained with Guava® Cell Cycle Reagent (Millipore), and cell cycle populations were determined by using the Guava® EasyCyte system (Millipore) according to the manufacturer's recommendations. The Guava® Cell Cycle software (Millipore) was used to determine the cell populations in the different cell cycle phases.

Trypan Blue Exclusion Assay—Cells were harvested by trypsinization, washed with PBS, and mixed with 0.5% trypan blue (Nacalai Tesque). After 3 min of equilibration, the cells were counted under a microscope.

Immunofluorescence—MCF-7 cells were reverse-transfected with control or NML siRNA and incubated for 48 h and then incubated in media containing various glucose concentrations (1000, 100, or 0 mg/liter) for 24 h. Cells were fixed with 4% paraformaldehyde at room temperature for 15 min and permeabilized with 0.5%Triton X-100 buffer (20 mM HEPES, 150 mM KCl, 0.5% Triton X-100) for 10 min at room temperature. Samples were blocked with 0.5% goat serum for 1 h, washed with PBS (140 mM NaCl, 2.7 mM KCl, 1.5 mM KH_2PO_4, and 8.1 mM Na_2HPO_4), and incubated with the indicated antibody for 2 h. Cells were washed with PBS and incubated with Alexa Fluor® 488 goat anti-mouse IgG (H+L) (Invitrogen) or Alexa Fluor® 594 goat anti-rabbit IgG (H+L) (Invitrogen) for 1 h. Cells were washed again with PBS, stained with 4, 6-diamidino-2-phenylindole (DAPI) (Dojindo), and mounted on slides with Vectashield (Vector Laboratories). Immunofluorescence was performed using Biozero immunofluorescence microscopy (Keyence, Osaka, Japan).

Immunoblotting—For immunoblotting, cells were harvested by trypsinization, washed with PBS, and lysed in radioimmune precipitation assay buffer (25 mM Tris-HCl, pH 7.6, 150 mM NaCl, 1% Nonidet P-40, 1% Triton X-100, 1% sodium deoxycholate, and 0.1% SDS) plus protease inhibitor mixture (Nacalaitesque) for 30 min on ice. Lysates were cleared by centrifugation at 16100 $\times$ *g* for 30 min at 4 °C. Protein concentrations were evaluated with a BCA kit (Thermo Scientific). Extracted proteins were separated by SDS-PAGE, transferred onto PVDF membranes (Millipore). After blocking with 5% skim milk in TBS-T buffer (20 mM Tris at pH 7.5, 150 mM NaCl, and 0.05% Tween 20) for 1 h, the membranes were incubated with the first antibody for 1 h. After washing with TBS-T buffer, the membranes were incubated with horseradish peroxidase-conjugated secondary antibody for 1 h. Bands were detected with Chemi-Lumi One (Nacalai Tesque) or Immobilon Western blotting detection kit (Millipore).

Immunoprecipitation—For immunoprecipitation of the endogenous proteins, MCF-7 cells were lysed in TNE buffer (20 mM Tris-HCl at pH 7.4, 150 mM NaCl, 2 mM EDTA, and 0.5% Nonidet P-40) at 4 °C for 30 min. The cleared lysate was incubated for 4 h with 2 μg of antibodies against the indicated proteins, 10 μl of protein G-Sepharose was added, and the sample was rotated for 2 h at 4 °C. After washing four times with the same buffer, immunoprecipitates were separated by SDS-PAGE and analyzed by immunoblotting with the indicated antibodies.

Antibodies—The antibodies used in these experiments were: β-Actin (Sigma), p53 (DO-1, Santa Cruz Biotechnology, Santa Cruz, CA), anti-FLAG M2 antibody (Sigma), phospho-p53 (Ser-15, Cell Signaling Technology, Beverly, MA), Acethyl-p53 (lysine 382, Cell Signaling Technology), p21 (F-5, Santa Cruz Biotechnology), Hdm2 (SMP14, Santa Cruz Biotechnology), PUMA (Cell Signaling Technology), AMPKα (Cell Signaling Technology), phospho-AMPKα (Thr172, Cell Signaling Technology), phosphoacetyl-CoA carboxylase (Cell Signaling Technology), p300 (N-15, Santa Cruz Biotechnology), upstream binding factor (UBF; Santa Cruz Biotechnology). Rabbit anti-human-MYBBP1A antibody was raised against a synthetic peptide corresponding to 1265–1328 amino acids of human-MYBBP1A. Rabbit anti-mouse-Mybbp1a antibody was raised against a synthetic peptide corresponding to 5–18 and 1321–1334 amino acids of mouse-Mybbp1a. NML antibody was prepared as described Murayama *et al.* (7).

RNA Purification and RT-Quantitative PCR—Total RNA was isolated with the FastPure® RNA kit (TAKARA) according to the manufacturer's instruction. Total RNA (1 μg) was

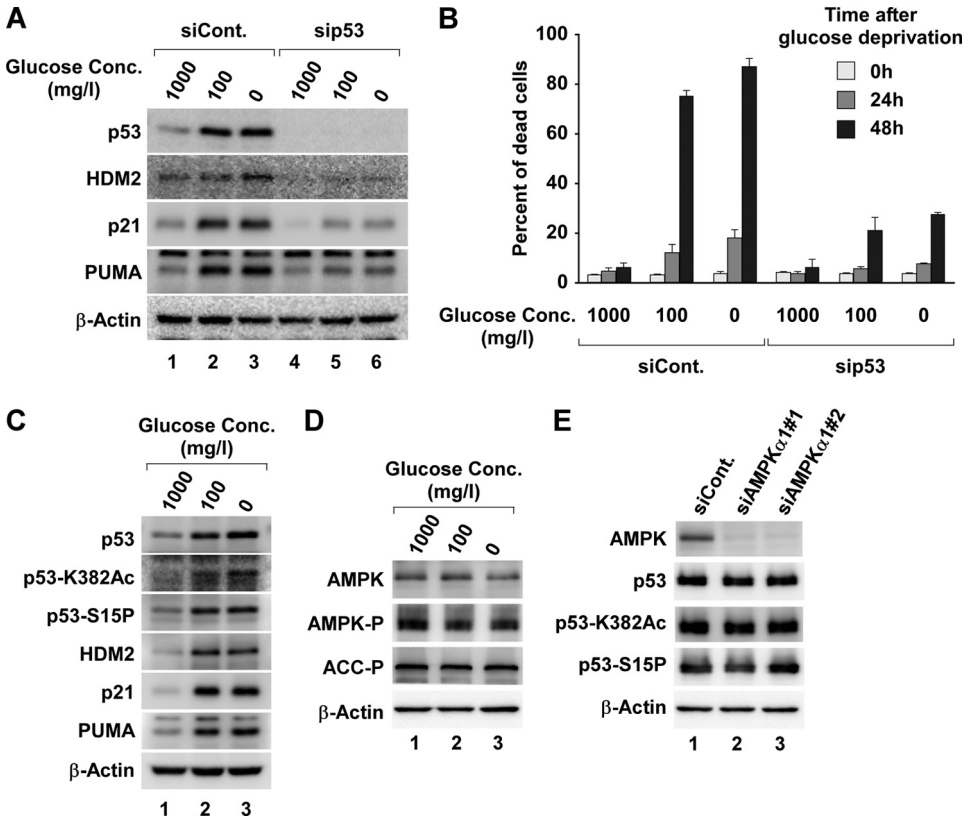

FIGURE 1. **Glucose limitation causes AMPK-independent p53 activation and induces cell death.** *A*, MCF-7 cells were treated with control siRNA or siRNA for p53 for 48 h and then incubated in media containing various glucose concentrations (1000, 100, or 0 mg/liter) for 24 h. The cell lysates prepared from these cells were immunoblotted using the indicated antibodies. *B*, MCF-7 cells were treated with control siRNA or siRNA for p53 for 48 h and then incubated in media containing various glucose concentrations for the indicated times. The percentage of dead cells was analyzed by a trypan blue exclusion assay. Values are the mean ± S.D., $n = 3$. *C*, the cell lysates prepared from MCF-7 cells incubated in various glucose concentrations for 24 h were analyzed by immunoblotting with the indicated antibodies. *ACC-P*, phospho- acetyl-CoA carboxylase *D*, MCF-7 cells were incubated in media containing various glucose concentrations for 24 h. The cell lysates prepared from these cells were immunoblotted using the indicated antibodies. ACC-P, phosphoacetyl-CoA carboxylase. *E*, MCF-7 cells were transfected with control siRNA or two independent siRNAs for AMPKα1 for 48 h and then cultured in medium without glucose for 24 h. The cell lysates were analyzed by immunoblotting.

reverse-transcribed with PrimeScript® 1st strand cDNA Synthesis kit (TAKARA). Real-time quantitative PCR analysis was performed using the Thermal Cycler Dice TP800 (Takara) and Platinum SYBR Green qPCR SuperMix-UDG (Invitrogen) as described in Murayama *et al.* (7). For PCR amplification, the specific primers 5′-ATCGTCCACCGCAAATGCTTCTA-3′ and 5′-AGCCATGCCAATCTCATCTTGTT-3′ for β-actin, 5′-GAACGGTGGTGTGTCGTTC-3′, and 5′-GCGTCTCGTCTCGTCTCACT-3′ for pre-rRNA were used.

Nucleoli Purification and Quantitative Determination of Nucleolar RNA Content—Nucleoli were isolated from 1.2×10^7 MCF-7 cells in high purify by density gradient fractionation as previously described Andersen *et al.* (21). Total nucleolar RNA was prepared from the isolated nucleoli and quantified by spectrometry.

RESULTS

Glucose Limitation Causes Cell Death in a p53-dependent Manner—p53 is reportedly activated in response to glucose limitation (6, 22, 23). To confirm this, we analyzed cell lysates from MCF-7 cells, which express wild type p53, cultured in various glucose concentrations by immunoblotting. We found that the protein levels of p53 and its downstream gene products, such as p21, HDM2, and PUMA, increased when glucose concentration was reduced (Fig. 1*A*). The induction of p53 downstream gene products was abrogated when p53 level was depleted by siRNA (Fig. 1*A*). Next, we tested whether the glucose limitation affected the viability of MCF-7 cells. A trypan blue exclusion assay indicated that glucose deprivation increased the percentage of dead cells. Furthermore, this was abrogated by p53 depletion (Fig. 1*B*). These results indicate that p53 is involved in cell death under nutrient stress. Then we analyzed the modification of p53 and found that Ser-15 phosphorylation and Lys-382 acetylation were stimulated in cells deprived of glucose (Fig. 1*C*).

Next, we investigated the mechanism underlying the activation of p53 in response to glucose starvation in MCF-7 cells. AMPK is responsible for the phosphorylation of p53 under low glucose conditions (6, 22). Therefore, we tested the effect of glucose deprivation on the phosphorylation of AMPK itself and that of AMPK substrate acetyl-CoA carboxylase. Glucose limitation did not affect AMPK phosphorylation or acetyl-CoA carboxylase phosphorylation in MCF-7 cells (Fig. 1*D*). Moreover, depletion of AMPKα1 by siRNA did not affect the levels of p53, p53 phosphorylation, and p53 acetylation increased by glucose deprivation (Fig. 1*E*). These results suggest that AMPK is not involved in the activation of p53 in response to glucose deprivation in MCF-7 cells under our experimental conditions.

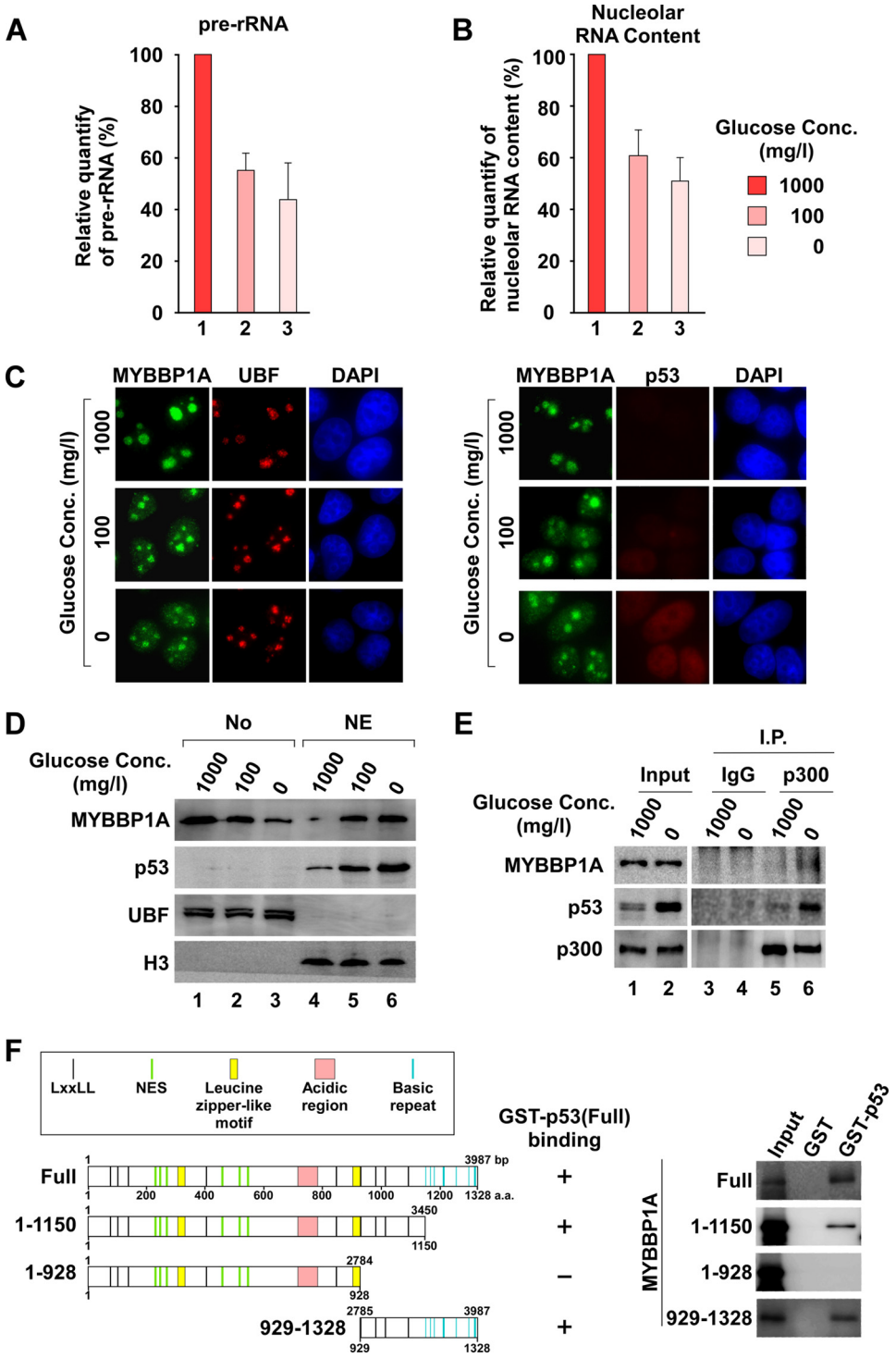

FIGURE 2. **Glucose limitation reduces nucleolar RNA content and causes MYBBP1A translocation into the nucleoplasm.** *A*, MCF-7 cells were incubated in media containing the indicated glucose concentrations for 24 h, and pre-rRNA levels were determined by RT-quantitative PCR using primers that are specific for the 5′ external transcribed spacer of pre-rRNA and normalized for cell count. The level of the cells cultured in medium containing 1000 mg/liter glucose was normalized to 100%. Values are the mean ± S.D., $n = 3$. *B*, nucleolar RNA was isolated from the purified nucleoli of MCF-7 cells cultured for 24 h in media containing the indicated glucose concentrations. Total nucleolar RNA levels were quantified by spectrophotometry. The level of the cells cultured in medium containing 1000 mg/liter glucose was normalized to 100%. Values are the mean ± S.D., $n = 3$. *C*, MCF-7 cells were cultured in media with the indicated glucose concentrations for 24 h, and the cells were stained using the indicated antibodies or DAPI (picture). *D*, MCF-7 cells were cultured in media with the indicated glucose concentrations for 24 h. The cells were fractionated into nucleolar (*NO*) and nuclear (*NE*) fractions, and proteins of each fraction were analyzed using indicated antibodies. UBF and histone H3 were shown as a loading control for nucleolar and nuclear fractions, respectively. *E*, MCF-7 cells were cultured in media with a glucose concentration of 1000 or 0 mg/liter for 24 h. The cell lysates were prepared, immunoprecipitated (*I.P.*) with normal rabbit IgG (*IgG*) or anti-p300 antibodies (*p300*), and analyzed by immunoblotting using the indicated antibodies. *F*, *in vitro* translated FLAG-HA-MYBBP1A full-length and deletion mutants (*left*) were incubated with GST-fused p53. After extensive washes, bound proteins were analyzed by immunoblot using HA antibodies (*right*). Conserved motifs in MYBBP1A are shown in *upper box*. *NES*, nuclear export signal.

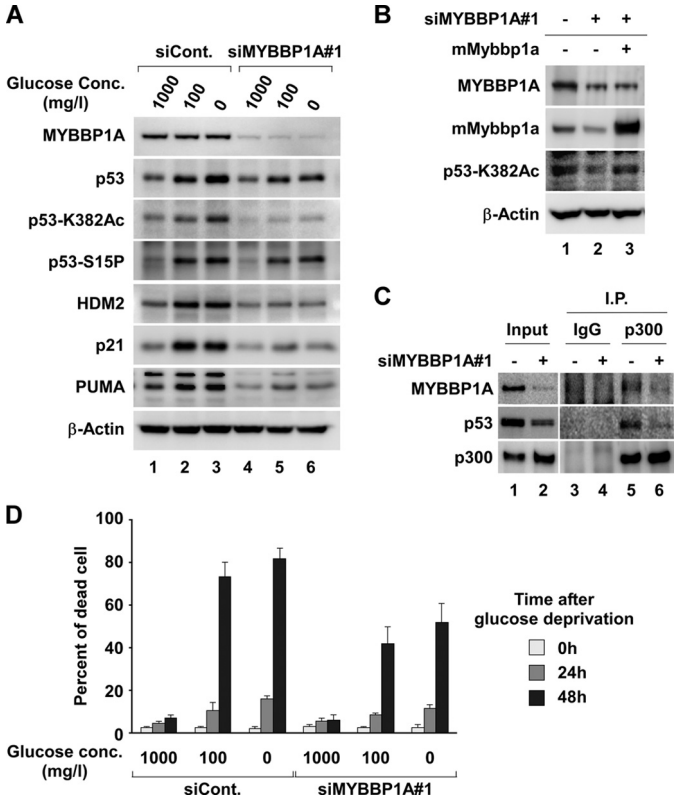

FIGURE 3. **Glucose limitation enhances acetylation and accumulation of p53 in a MYBBP1A-dependent manner.** *A*, MCF-7 cells were treated with control siRNA or siRNA for MYBBP1A#1 for 48 h and then incubated in media containing various glucose concentrations (1000, 100, or 0 mg/liter) for 24 h. The cell lysates prepared from these cells were immunoblotted using the indicated antibodies. *B*, MCF-7 cells were treated with control siRNA or siRNA for MYBBP1A#1 and transfected with mouse-MYBBP1A. Thirty-six hours after transfection, cells were cultured in medium without glucose for 24 h. The cell lysates prepared from these cells were immunoblotted using the indicated antibodies. Mouse-Mybbp1a (*mMybbp1a*) antibody cross-reacts with human-MYBBP1A. *C*, MCF-7 cells were transfected with control siRNA or siRNA for MYBBP1A#1 for 48 h and then cultured in medium without glucose for 24 h. The cell lysates were prepared, immunoprecipitated (*I.P.*) with normal rabbit IgG (IgG) or anti-p300 antibodies (p300), and analyzed by immunoblotting using the indicated antibodies. *D*, MCF-7 cells were transfected with control siRNA or siRNA for MYBBP1A#1 for 48 h and then cultured in media containing various glucose concentrations for the times indicated. The percentage of dead cells was analyzed using a trypan blue exclusion assay. Values are the mean ± S.D., $n = 3$.

Therefore, a pathway(s) other than the LKB1-AMPK pathway may be involved in the up-regulation of p53 when glucose concentration is reduced in MCF-7 cells.

MYBBP1A Is Implicated in the Activation of p53 in Response to Glucose Limitation—Our recent work revealed that the nucleolar protein MYBBP1A activates p53 when ribosomal biogenesis was suppressed. MYBBP1A, which is anchored to the nucleolus by RNA, translocated from the nucleolus to the nucleoplasm when nucleolar RNA content was reduced by inhibition of rRNA transcription. The translocated MYBBP1A acetylates and accumulates p53 by facilitating the interaction between p53 and p300 (27).

Glucose starvation reduces ribosomal biogenesis (1, 7). Therefore, the reduction in nucleolar RNA content in response to glucose starvation may cause the translocation of MYBBP1A, which eventually leads to the activation of p53. To test this possibility, we first examined whether glucose starvation reduced rRNA transcription in MCF-7 cells. As shown in Fig. 2*A*, rRNA transcription was reduced when glucose concentration was decreased. Nucleolar RNA content also reduced in parallel with the reduction in rRNA transcription (Fig. 2*B*). We next examined the effect of glucose starvation on the localization of MYBBP1A. MYBBP1A localized dominantly in the nucleolus when cells were cultured in medium containing normal glucose concentration (1000 mg/liter) (Fig. 2*C*). However, MYBBP1A translocated from the nucleolus to the nucleoplasm in response to glucose starvation, whereas another nucleolar protein UBF remained in the nucleolus (Fig. 2*C*, *left*; 100 or 0 mg/liter). Moreover, MYBBP1A and p53 localized diffusely in the nucleoplasm under glucose-starved conditions (Fig. 2*C*, *right*; 100 or 0 mg/liter). The subcellular fractionation experiment confirmed the translocation of MYBBP1A (Fig. 2*D*). This quantitative assay showed that translocation of MYBBP1A to the nucleoplasm paralleled the reduction in nucleolar RNA content.

Then we tested the interaction between p300 and p53 because we have already established that the translocated MYBBP1A strengthened their interactions (27). We immunoprecipitated p300 from MCF-7 cell extracts cultured in medium with or without glucose followed by immunoblotting. As shown in Fig. 2*E*, increasing amounts of p53 proteins were detected in the immunoprecipitants of p300. This result indicates that the interaction between p53, p300, and MYBBP1A is increased under glucose-starved conditions. Moreover, the GST pulldown experiment showed that p53 interacts with 929–1150 amino acid residues of MYBBP1A (Fig. 2*F*).

Next, we tested whether MYBBP1A was implicated in the activation of p53 in response to glucose deprivation by knockdown of MYBBP1A. siRNA mediated-MYBBP1A depletion almost abolished the enhancement of p53 acetylation induced by glucose starvation and partly suppressed the accumulation of p53 protein (Fig. 3*A* and supplemental Fig. 1*A*). Up-regulation of p53 downstream gene products, such as p21 and PUMA, under low glucose conditions was also compromised by the depletion of MYBBP1A (Fig. 3*A* and supplemental Fig. 1*A*). In contrast, phosphorylation of p53 was barely influenced by this treatment (Figs. 3*A* and supplemental Fig. 1*A*). Moreover, re-expression of MYBBP1A in the MYBBP1A-depleted cells restored the acetylation of p53 under glucose-starved conditions (Fig. 3*B*). Thus, MYBBP1A probably contributes to nutrient stress-induced p53 activation not by affecting its phosphorylation but by enhancing its acetylation. Consistent with this phenomenon, depletion of MYBBP1A abolished the enhanced interaction between p53 and p300 under glucose-starved conditions (Fig. 3*C*). Taken together, we consider that glucose starvation induces the translocation of MYBBP1A from the nucleolus to the nucleoplasm, where it stabilizes the interaction between p300 and p53, which causes acetylation and accumulation of p53. Then we tested whether MYBBP1A was required to induce cell death in response to glucose starvation. As expected, depletion of MYBBP1A reduced the percentage of dead cells (Figs. 3*D* and supplemental Fig. 1*B*), indicating the involvement of p53 in cell death induced by low glucose concentration.

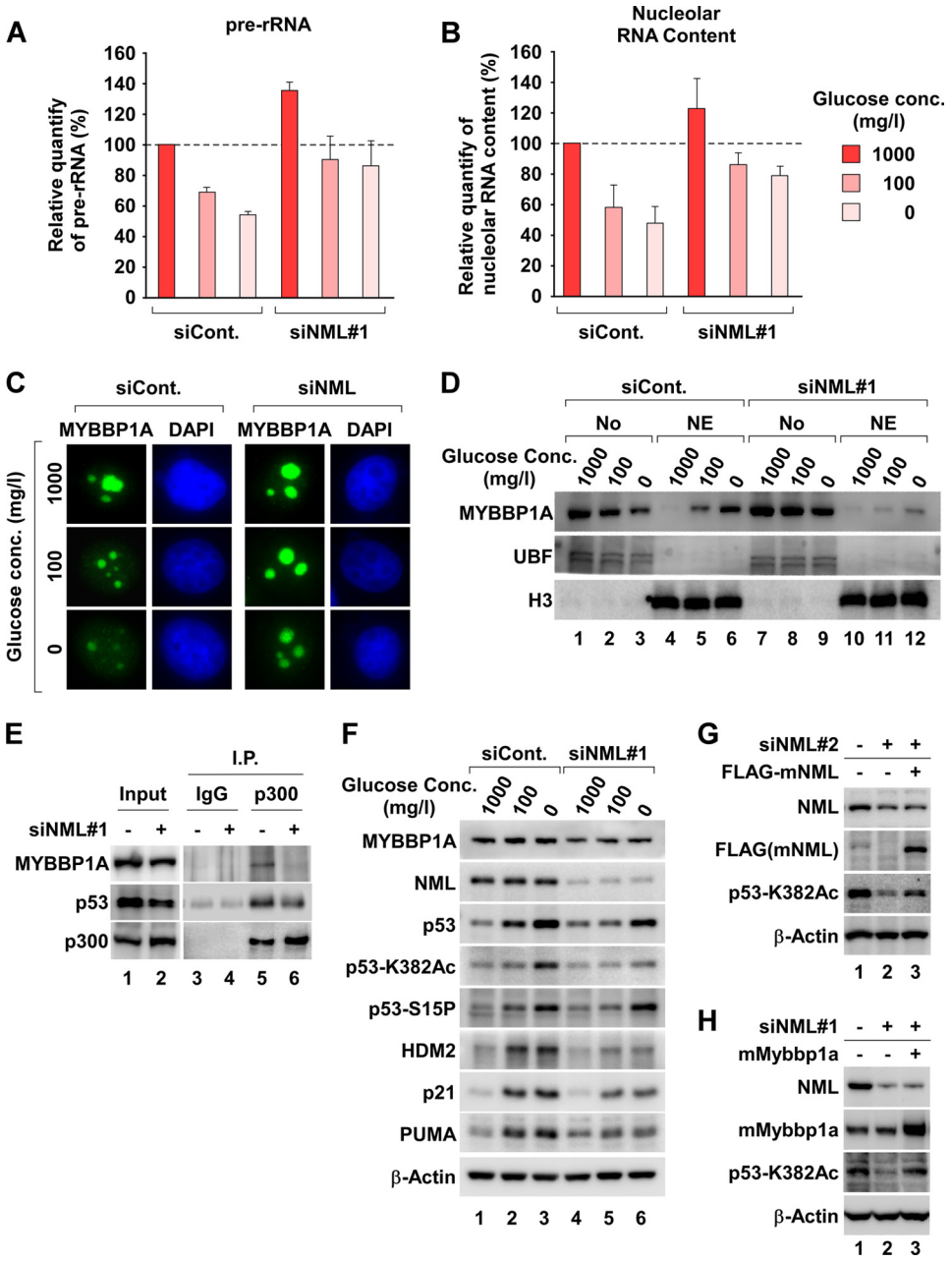

FIGURE 4. **NML is involved in the activation of p53 in response to glucose limitation.** *A*, MCF-7 cells transfected with control siRNA or siRNA for NML#1 for 48 h were cultured in media containing the indicated glucose concentrations for 24 h. The pre-rRNA levels were determined by RT-quantitative PCR and normalized for cell count. The level of the cells transfected with control siRNA and cultured in medium containing 1000 mg/liter glucose was normalized to 100%. Values are the mean ± S.D., $n = 3$. *B*, nucleolar RNA was isolated from the purified nucleoli of the same set of MCF-7 cells as *A*. Total nucleolar RNA levels were quantified by spectrophotometry. The levels of the cells transfected with control siRNA and cultured in medium containing 1000 mg/liter glucose was normalized to 100%. Values are the mean ± S.D., $n = 3$. *C*, MCF-7 cells transfected with control siRNA or siRNA for NML for 48 h were cultured in media with the indicated glucose concentrations for 24 h, and the cells were stained by the indicated antibodies or DAPI (picture). *D*, MCF-7 cells were treated with control siRNA or siRNA for NML#1 for 48 h and then incubated in media containing indicated glucose concentrations for 24 h. The cells were fractionated into nucleolar (*NO*) and nuclear (*NE*) fractions, and proteins of each fraction were analyzed using indicated antibodies. UBF and histone H3 were shown as a loading control for nucleolar and nuclear fraction, respectively. *E*, MCF-7 cells were transfected with control siRNA or siRNA for NML#1 for 48 h and then cultured in medium without glucose for 24 h. The cell lysates were prepared, immunoprecipitated (*I.P.*) with normal rabbit IgG (IgG) or anti-p300 antibodies (p300), and analyzed by immunoblotting using the indicated antibodies. *F*, MCF-7 cells were treated with control or siRNA for NML#1 for 48 h and then incubated in media containing indicated glucose concentrations for 24 h. The cell lysates prepared from these cells were immunoblotted using the indicated antibodies. *G*, MCF-7 cells were treated with control siRNA or siRNA for NML#2 and transfected with mouse-NML. Thirty-six hours after transfection, cells were cultured in medium without glucose for 24 h. The cell lysates prepared from these cells were immunoblotted using the indicated antibodies. We used siRNA#2 in this experiment because siRNA#1 targeted mouse-NML as well as human-NML. *H*, MCF-7 cells were treated with control siRNA or siRNA for NML#1 and transfected with mouse-MYBBP1A. Thirty-six hours after transfection, cells were cultured in medium without glucose for 24 h. The cell lysates prepared from these cells were immunoblotted using the indicated antibodies. Mouse-Mybbp1a (*mMybbp1a*) antibody cross-reacts with human-MYBBP1A.

NML Is Implicated in the Activation of p53 in Response to Glucose Limitation—We recently reported that the novel nucleolar protein NML formed a protein complex (eNoSC) with SIRT1 and SUV39H1 and suppressed rRNA transcription in response to glucose starvation (7). Thus, NML probably regulates p53 activation as follows. First, NML reduces

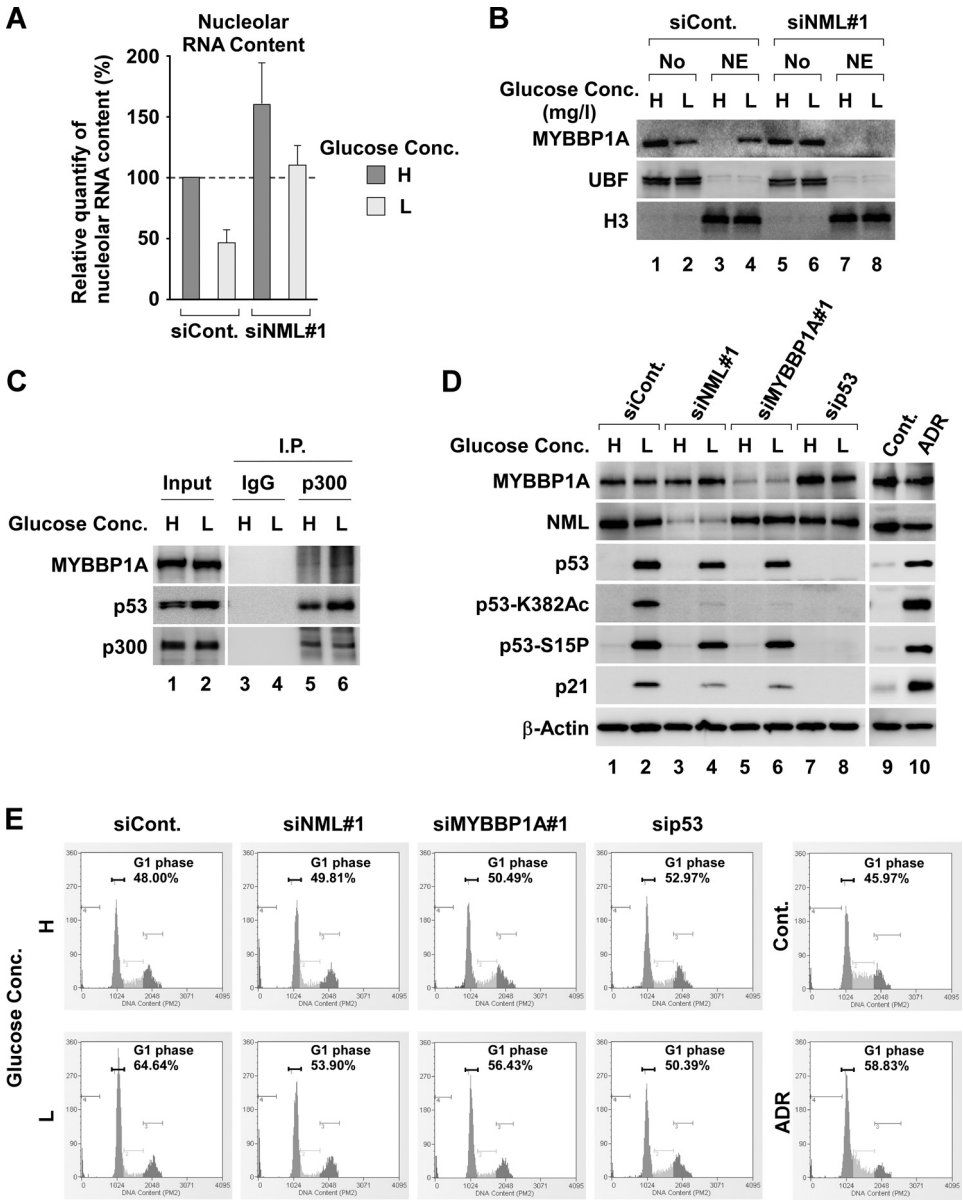

FIGURE 5. **NML-MYBBP1A promotes G_1 cell cycle arrest in response to glucose limitation.** *A*, WI-38 cells transfected with the control siRNA or siRNA for NML#1 for 36 h were cultured in media containing 4500 mg/liter (*H*) or 300 mg/liter (*L*) glucose for 60 h. Nucleolar RNA levels were quantified by spectrophotometry. The levels of the cells transfected with control siRNA and cultured in medium containing 4500 mg/liter glucose was normalized to 100%. Values are the mean ± S.D., $n = 3$. *B*, WI-38 cells were treated with the indicated siRNAs for 36 h and then incubated in media containing 4500 mg/liter (*H*) or 300 mg/liter (*L*) glucose for 60 h. The nucleolar and nuclear extract (*NO* and *NE*, respectively) were analyzed by immunoblotting using the indicated antibodies. UBF and histone H3 were shown as a loading control for nucleolar and nuclear fraction, respectively. *C*, WI-38 cells were cultured in media containing 4500 mg/liter (*H*) or 300 mg/liter (*L*) glucose for 60 h. The cell lysates were prepared, immunoprecipitated (*I.P.*) with normal rabbit IgG (IgG) or anti-p300 antibodies (p300), and analyzed by immunoblotting using the indicated antibodies. *D*, WI-38 cells transfected with the indicated siRNAs for 36 h were cultured in media containing 4500 mg/liter (H) or 300 mg/liter (L) glucose for 60 h. The cell lysates prepared from these cells were immunoblotted using the antibodies indicated. Adriamycin (*ADR*)-treated cells were used as a positive control for p53 activation. *E*, the DNA contents of the same set of WI-38 cells as *D* were determined by FACS analysis. The percentages of the G_1 phase cells were 48.00 ± 5.02% (*siCont*, *H*). 49.81 ± 1.33% (*siNML*, *H*), 50.49 ± 2.44% (*siMYBBP1A*, *H*), 52.97 ± 3.07% (*sip53*, *H*), 64.64 ± 2.77% (*siCont*, *L*), 53.90 ± 4.17% (*siNML*, *L*), 56.43 ± 3.72% (*siMYBBP1A*, *L*), and 50.39 ± 4.12% (*sip53*, *L*). The DNA contents of adriamycin-treated cells are shown in parallel; 45.97 ± 2.30% (*Cont.*); 58.83 ± 5.32% (*ADR*).

rRNA transcription by glucose starvation, which leads to the reduction in nucleolar RNA content. Next, as a consequence of the reduced nucleolar RNA content, MYBBP1A translocates from the nucleolus to the nucleoplasm. The translocated MYBBP1A strengthens the interaction between p53 and p300, resulting in the stimulation and activation of p53.

To address this possibility, we first examined whether NML was required for the reduction of both rRNA transcription and nucleolar RNA content under low glucose conditions in MCF-7 cells. Our experimental results indicate that the reductions in rRNA transcription and nucleolar RNA content were alleviated by NML depletion (Figs. 4, *A* and *B*, and supplemental Fig. 1*C*, respectively). Next we tested the effect of NML depletion on the localization of MYBBP1A (Fig. 4, *C* and *D*, and supplemental Fig. 1*D*). Immunofluorescence staining and immunoblotting experiments indicated that the translocation of MYBBP1A into the nucleoplasm in response to glucose limitation was weak-

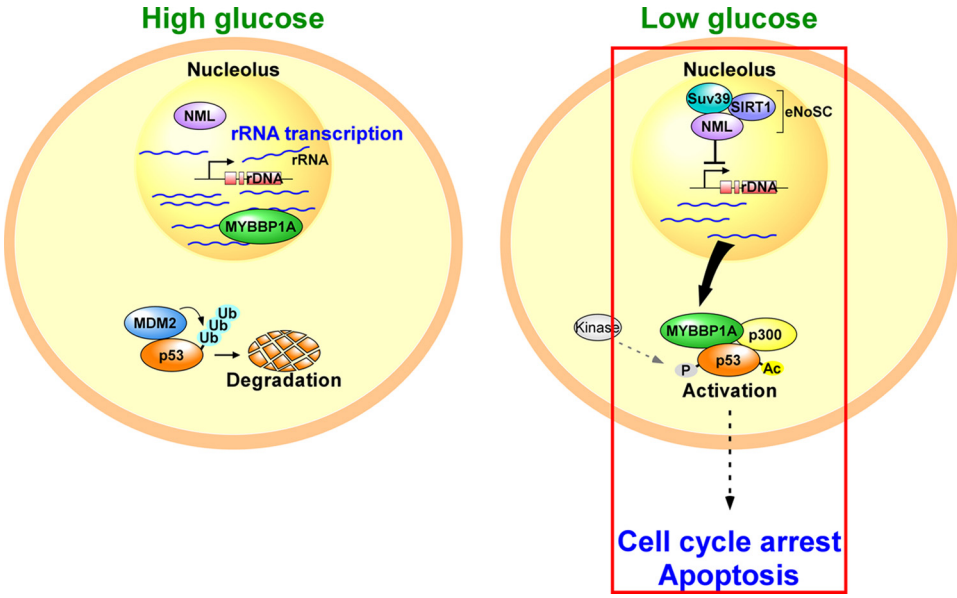

FIGURE 6. **A model for p53 activation by NML-MYBBP1A in response to glucose limitation.** See "Discussion." *Ub*, ubiquitination; *P*, phosphorylation; *Ac*, acetylation.

ened by the depletion of NML (Fig. 4, *C* and *D*, and supplemental Fig. 1*D*). Consistent with this result, the enhancement of the interaction between p53 and p300 by glucose starvation was not observed when NML was depleted (Fig. 4*E*). Finally, we tested the effect of NML on p53 activation. NML depletion efficiently abolished the enhancement of p53 acetylation in response to glucose starvation without affecting the phosphorylation of p53; this was similar to the case of MYBBP1A depletion (Fig. 4*F* and supplemental Fig. 1*E*). Up-regulation of p53 downstream gene products in glucose-starved conditions was also weakened by the depletion of NML (Figs. 4*F* and supplemental Fig. 1*E*). Re-expression of NML in NML-depleted cells restored the acetylation of p53 under glucose-starved conditions (Fig. 4*G*). MYBBP1A overexpression salvaged the NML-knockdown phenotype (Fig. 4*H*). This result supports the idea that MYBBP1A and NML function to activate p53 in the same pathway. Thus, NML contributes to p53 acetylation and activation by promoting MYBBP1A translocation into the nucleoplasm as a consequence of reduced nucleolar RNA content under the glucose-starved conditions.

NML-MYBBP1A Pathway Is Involved in Cell Cycle Arrest upon Glucose Deprivation—In this study we found that the NML-MYBBP1A pathway contributes to p53 activation in response to glucose deprivation. To assess the physiological role of NML-MYBBP1A-mediated p53 activation in normal cells, we used a human normal fibroblast cell line, WI-38. As shown in Fig. 5*A*, glucose limitation-caused reductions in nucleolar RNA content were also alleviated by NML depletion in normal cells. Next, we tested the effect of NML depletion on the localization of MYBBP1A (Fig. 5*B*). Immunoblotting experiments showed that the translocation of MYBBP1A into the nucleoplasm in response to glucose limitation was weakened by the depletion of NML (Fig. 5*B*). Moreover, translocated MYBBP1A interacted with p53 and p300 (Fig. 5*C*). Next, we treated WI-38 cells with the control siRNA or siRNA for NML, MYBBP1A, or p53 and then cultured them in media containing high (*H*; 4500 mg/liter) or low (*L*; 300 mg/liter) glucose and tested the activation of p53 (Fig. 5*D*). Upon glucose starvation, p53 was acetylated, and the p53 downstream gene product p21 increased (Fig. 5*D*). The up-regulation of p53 acetylation and induction of p21 was reduced by siRNA treatment for NML or MYBBP1A (Fig. 5*D*). These results indicate that the NML-MYBBP1A pathway is involved in p53 activation in response to glucose starvation in normal as well as cancer cells. Next, we tested the effect of the NML-MYBBP1A pathway on cell proliferation under glucose-starved conditions (Fig. 5*E*). FACS analysis indicated that WI-38 cells were arrested in the G_1 phase in medium containing low glucose (Fig. 5*E*). This enhancement of G_1 cell cycle arrest was abolished when p53 was depleted (Fig. 5*E*). A similar phenotype was observed on depletion of NML or MYBBP1A (Fig. 5*E*). These results suggest that the NML-MYBBP1A pathway contributes to G_1 cell cycle arrest by activating p53 in normal WI-38 cells when glucose concentration is reduced, which may contribute to limiting energy consumption under glucose starvation.

DISCUSSION

Here we have focused on the novel function of the nucleolus that converts the signal of intracellular energy shortage into activation of p53. Two nucleolar factors are involved in this regulation. The first is the NML-SITR1-SUV39H1 protein complex eNoSC that detects intracellular energy status in terms of the NAD^+/NADH ratio. Upon energy shortage, indicated by an increased NAD^+/NADH ratio, eNoSC is activated via its SIRT1 subunit and suppresses rRNA transcription, which eventually leads to the reduction in nucleolar RNA content. The second is MYBBP1A that is tethered to the nucleolus by binding to nucleolar RNA. MYBBP1A translocates from the nucleolus to the nucleoplasm when nucleolar RNA content is reduced. The translocated MYBBP1A enhances the acetylation and accumulation of p53 by enhancing the interaction between p53 and p300 (27). Thus, eNoSC functions as a detector and a

signal transducer of the intracellular energy status, whereas MYBBP1A functions as an effector that activates p53 by enhancing its acetylation (Fig. 6).

In addition to the NML-MYBBP1A pathway, the LKB1-AMPK pathway is reportedly implicated in this regulation. Namely, in response to intracellular energy shortage, the increased AMP/ATP ratio activates AMPK, which leads to suppression of ribosomal biogenesis by inhibiting mTOR/p70 S6 kinase activity (3). In addition, activated AMPK enhances phosphorylation of p53 at its Ser-15 and Ser-46 residues, leading to p53 activation (6, 22).

The biological significance and separate roles of the NML-MYBBP1A and LKB1-AMPK pathways remain to be determined. However, these two pathways may compensate for each other, thus, improving their efficiency and reliability.

The suppression of ribosomal biogenesis or rRNA transcription by the LKB1-AMPK or NML-MYBBP1A pathways in response to energy deprivation is considered to be an adaptation mechanism that reduces energy expenditure. In addition, these pathways activate p53 under energy-starved conditions. However, the physiological relevance of p53 up-regulation upon energy starvation is enigmatic. For example, our experimental results using WI-38, a human normal fibroblast cell line, indicate that up-regulation of p53 in response to glucose starvation leads to G_1 cell cycle arrest. Thus, the NML-MYBBP1A pathway reduces the energy consumption of WI-38 by repressing ribosomal biogenesis as well as arresting the cell cycle in the G_1 phase. In contrast, our experimental results using MCF-7, a human breast tumor cell line, showed that glucose limitation induced cell death in a p53-dependent manner. The molecular basis underlying this controversy on the role of p53 on cell fate remains to be determined. Notably, the acetylation of p53 reportedly enhances sequence-specific DNA binding of p53 and recruitment of a coactivator complex to promoter regions to activate p53-target gene expression (24, 25). The functional consequences of p53 acetylation suggest that the strength of acetylation may determine p53 regulation and cell fate. The activation of genes involved in cell cycle control requires partial acetylation, whereas the activation of proapoptotic genes requires full activation of p53 (26). Furthermore, we found that the amount of MYBBP1A in the normal cell line is less than that in the cancer cell line (data not shown). The differences in cell fate due to activation of p53 between cell lines (*e.g.* normal cells *versus* tumor cells) may be explained by the difference in the expression levels of MYBBP1A.

REFERENCES

1. Hoppe, S., Bierhoff, H., Cado, I., Weber, A., Tiebe, M., Grummt, I., and Voit, R. (2009) *Proc. Natl. Acad. Sci. U.S.A.* **106,** 17781–17786
2. Bhaskar, P. T., and Hay, N. (2007) *Dev. Cell* **12,** 487–502
3. Hardie, D. G. (2004) *J. Cell Sci.* **117,** 5479–5487
4. Inoki, K., Zhu, T., and Guan, K. L. (2003) *Cell* **115,** 577–590
5. Shaw, R. J., Kosmatka, M., Bardeesy, N., Hurley, R. L., Witters, L. A., DePinho, R. A., and Cantley, L. C. (2004) *Proc. Natl. Acad. Sci. U.S.A.* **101,** 3329–3335
6. Jones, R. G., Plas, D. R., Kubek, S., Buzzai, M., Mu, J., Xu, Y., Birnbaum, M. J., and Thompson, C. B. (2005) *Mol. Cell* **18,** 283–293
7. Murayama, A., Ohmori, K., Fujimura, A., Minami, H., Yasuzawa-Tanaka, K., Kuroda, T., Oie, S., Daitoku, H., Okuwaki, M., Nagata, K., Fukamizu, A., Kimura, K., Shimizu, T., and Yanagisawa, J. (2008) *Cell* **133,** 627–639
8. Levine, A. J. (1997) *Cell* **88,** 323–331
9. Rubbi, C. P., and Milner, J. (2003) *EMBO J.* **22,** 6068–6077
10. Boisvert, F. M., van Koningsbruggen, S., Navascués, J., and Lamond, A. I. (2007) *Nat. Rev. Mol. Cell Biol.* **8,** 574–585
11. Prives, C., and Hall, P. A. (1999) *J. Pathol.* **187,** 112–126
12. Castle, C. D., Cassimere, E. K., Lee, J., and Denicourt, C. (2010) *Mol. Cell. Biol.* **30,** 4404–4414
13. Hölzel, M., Orban, M., Hochstatter, J., Rohrmoser, M., Harasim, T., Malamoussi, A., Kremmer, E., Langst, G., and Eick, D. (2010) *J. Biol. Chem.* **285,** 6364–6370
14. McMahon, M., Ayllón, V., Panov, K. I., and O'Connor, R. (2010) *J. Biol. Chem.* **285,** 18309–18318
15. Yuan, X., Zhou, Y., Casanova, E., Chai, M., Kiss, E., Gröne, H. J., Schütz, G., and Grummt, I. (2005) *Mol. Cell* **19,** 77–87
16. Boulon, S., Westman, B. J., Hutten, S., Boisvert, F. M., and Lamond, A. I. (2010) *Mol. Cell* **40,** 216–227
17. Mayer, C., Bierhoff, H., and Grummt, I. (2005) *Genes Dev.* **19,** 933–941
18. Weber, J. D., Taylor, L. J., Roussel, M. F., Sherr, C. J., and Bar-Sagi, D. (1999) *Nat. Cell Biol.* **1,** 20–26
19. Honda, R., and Yasuda, H. (1999) *EMBO J.* **18,** 22–27
20. Lowe, S. W., and Sherr, C. J. (2003) *Curr. Opin. Genet. Dev.* **13,** 77–83
21. Andersen, J. S., Lam, Y. W., Leung, A. K., Ong, S. E., Lyon, C. E., Lamond, A. I., and Mann, M. (2005) *Nature* **433,** 77–83
22. Okoshi, R., Ozaki, T., Yamamoto, H., Ando, K., Koida, N., Ono, S., Koda, T., Kamijo, T., Nakagawara, A., and Kizaki, H. (2008) *J. Biol. Chem.* **283,** 3979–3987
23. Ide, T., Brown-Endres, L., Chu, K., Ongusaha, P. P., Ohtsuka, T., El-Deiry, W. S., Aaronson, S. A., and Lee, S. W. (2009) *Mol. Cell* **36,** 379–392
24. Gu, W., and Roeder, R. G. (1997) *Cell* **90,** 595–606
25. Luo, J., Li, M., Tang, Y., Laszkowska, M., Roeder, R. G., and Gu, W. (2004) *Proc. Natl. Acad. Sci. U.S.A.* **101,** 2259–2264
26. Kruse, J. P., and Gu, W. (2009) *Cell* **137,** 609–622
27. Kuroda, T. (2011) *EMBO J.* **30,** 1054–1066